

# Quantification of Frataxin-M Protein, a Blood Biomarker of the Rare Disease Friedreich's Ataxia

Using the Agilent 6495 triple quadrupole LC/MS system

## Authors

Nicolas Eskenazi,  
Teerapat Rojsajakul,  
Clementina Mesaros, and  
Ian A. Blair  
Penn/CHOP Friedreich's  
Ataxia Center of Excellence  
and Department of  
Systems Pharmacology and  
Translational Therapeutics,  
Perelman School of Medicine,  
University of Pennsylvania  
  
Linfeng Wu  
Agilent Technologies, Inc.

## Abstract

Friedreich's ataxia (FRDA) is an inherited disease involving progressive nervous system damage and movement problems caused by the deficient expression of mitochondrial mature frataxin (frataxin-M) protein. Frataxin-M (81-210) arises from a two-step proteolytic cleavage of full-length frataxin (1-210) by mitochondrial processing peptidase (MPP). Frataxin-M is not secreted into the circulation, and so cannot be analyzed in plasma or serum. But frataxin-M is present in blood cells such as platelets and human peripheral blood mononuclear cells (PBMCs) that possess mitochondria.

Mass spectrometry (MS) in combination with immunoprecipitation (IP) and stable isotope dilution methodology can quantify frataxin-M with high precision and accuracy. This quantification has primarily involved the use of high-resolution MS coupled with a nanoflow liquid chromatography (nanoflow LC) system, which is time-consuming and requires rigorous quality control to maintain the nanoflow LC/MS system. Standard-flow LC systems coupled with unit-resolution triple quadrupole LC/MS (LC/TQ) systems are not typically used for the quantification of low-abundance proteins such as frataxin-M. This application note shows that standard HPLC flow rates on the Agilent 6495 LC/TQ in multiple reaction monitoring (MRM) acquisition mode delivers better frataxin-M quantification analysis. The system delivers better sensitivity, precision, accuracy, and instrument run time when compared to a trap-and-elute nanoflow LC/MS system coupled with a high-resolution orbital trapping mass spectrometer in parallel reaction monitoring (PRM) acquisition mode. Therefore, the 6495 LC/TQ platform using standard flow HPLC is better suited than the trap-and-elute nanoflow LC/MS system for high-throughput frataxin-M quantification in blood samples.

## Introduction

Although FRDA is considered a rare disease, it is the most common hereditary ataxia in the US population. As a result of its progressive nature, most patients are wheelchair-bound by 15.5 ± 7.4 years (mean age ± SD) after the onset of disease.<sup>1</sup> However, heart disease is the major cause of death.<sup>2</sup> At present, there is no effective treatment for FRDA, although the NRF-2 activator omeveloxolone was found to be safe and to improve neurological function at the therapeutic dose, and so provides a potential future therapeutic strategy.<sup>3</sup> The genetic basis of most FRDA cases is a GAA triplet repeat expansion in the first intron of the frataxin (FXN) gene on both alleles (GAA1 and GAA2), which causes epigenetic transcriptional silencing and reduced expression of full-length frataxin protein.<sup>4</sup> A minority of FRDA patients (<3%) are compound heterozygotes possessing point or small mutations on one allele with a GAA repeat expansion on the other.<sup>5</sup> In a typical FRDA case, the length of GAA1 (the shortest expansion) correlates with disease severity, whereas longer GAA expansions result in earlier onset and a faster progression.<sup>6</sup> Human full-length frataxin (isoform 1, MW = 23,135 Da) is expressed as a 210 amino acid precursor protein with an N-terminal mitochondrial targeting sequence (Figure 1). A two-step proteolytic cleavage by mitochondrial processing peptidase (MPP) results in the formation of mitochondrial frataxin-M (81-210; MW = 14,268 Da). Several lines of evidence strongly suggest that frataxin-M is a functional component in a series of pathways including iron-sulfur cluster assembly, iron storage, heme biosynthesis, the respiratory chain, and cellular response to oxidative stress.<sup>7-10</sup> In contrast, extra-mitochondrial frataxin isoform E (frataxin-E) protein (76-210; MW = 14,953 Da) discovered in erythrocytes, lacks a

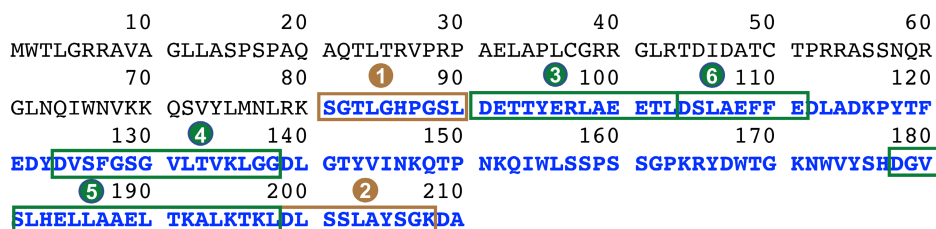


**Figure 1.** Amino acid sequences of full-length frataxin and frataxin-M (shown in blue). Asp-N digested peptides 1 and 2 (brown boxes) were used for quantification and peptides 3 to 5 (green boxes) were used for confirmation of protein detection.

mitochondrial targeting sequence. It arises through alternative splicing followed by N-terminal acetylation during translation;<sup>11</sup> its expression is downregulated in FRDA by DNA hypermethylation.<sup>12</sup> No function has yet been ascribed to frataxin-E.

Frataxin is not secreted into the circulation and so it cannot be analyzed in plasma or serum. Levels in the past were typically measured by Western blot analysis or enzyme-linked immunosorbent assay (ELISA) or electro-chemiluminescence from FRDA fibroblasts, lymphocytes, muscle biopsies, and PBMCs.<sup>13</sup> The discovery that frataxin-E is found exclusively in erythrocytes permits frataxin to be analyzed in whole blood samples rather than in individual cells such as platelets or PBMCs.<sup>14</sup> This discovery revealed that frataxin-M is located only in blood cells such as platelets and PBMCs that possess mitochondria. Furthermore, mass spectrometry (MS) with stable isotope dilution methods can quantify frataxin-M with high precision and accuracy. This analysis has primarily involved the use of nanoflow liquid chromatography separation coupled with high-resolution MS (nanoflow LC/MS), which is time-consuming and requires rigorous quality control and expertise to maintain the analytical instrument.<sup>13</sup> Disease and biomarker studies such as the one described in this study often require the analysis of larger sample cohorts to ensure statistically confident

findings, making throughput a critical consideration. Unit-resolution triple quadrupole instruments coupled with a standard-flow LC system (LC/TQ) are designed to be more robust and capable of higher throughput, especially in the context of larger cohort studies.

To determine whether a standard flow 6495 LC/TQ instrument could improve upon the current trap-and-elute nanoflow LC/MS system for routine quantification of frataxin-M, samples were run on both systems. The whole blood samples from FRDA subjects were spiked with a stable isotope analog of frataxin-M, then enriched by IP, which was followed by digestion with Asp-N protease. The digested peptides were analyzed on the two LC/MS instruments. The correlation coefficients for the linear standard curve regression lines, limits of detection (LODs), and lower limits of quantification (LLOQs) showed better results on the 6495 LC/TQ system. The results were achieved with less on-column sample loading than needed for the trap-and-elute-based nanoflow LC/MS system. In addition, there was a dramatic difference in the instrument run time on the two LC/MS platforms. This translated to an overall individual run time of 11 minutes on the 6495 LC/TQ system and 105 minutes on the nanoflow LC/MS system. Therefore, samples from a typical analysis of 10 controls and 30 FRDA subjects' blood samples could be completed within a single day instead of over 8 days, which was required for

the nanoflow LC/MS system. These data suggest that the standard flow 6495 LC/TQ platform is better suited than the trap-and-elute nanoflow LC/MS system for high throughput frataxin-M quantification in blood samples.

## Experimental

### Chemicals and materials

All reagents and solvents were LC/MS grade quality unless otherwise noted. [ $^{13}\text{C}_6$ ]-leucine was from Cambridge Isotope Laboratories (Andover, MA). Anti-frataxin antibody (clone 1D9) was from LifeSpan Biosciences, Inc. (Seattle, WA). Dimethyl pimelimidate dihydrochloride (DMP), ethylenediaminetetraacetic acid (EDTA), cOmplete Mini EDTA-free Easypack protease inhibitor cocktail tablets, endoproteinase Asp-N sequencing grade, DL-dithiothreitol (DTT), bovine serum albumin (BSA), human lysozyme, imidazole, glycerol, phenylmethylsulfonyl fluoride (PMSF), triethanolamine, ethanolamine, and M9, minimal salts, 5X powder, minimal microbial growth medium (M9 media) were purchased from MilliporeSigma (Billerica, MA). Ni-NTA agarose resin was purchased from Qiagen (Germantown, MD). HPLC grade water and acetonitrile were from Burdick and Jackson (Muskegon, MI). Ammonium bicarbonate and acetic acid were purchased from Fisher Scientific (Pittsburgh, PA). Protein G magnetic Dynabeads were obtained from Life Technologies Corporation (Grand Island, NY).

### Whole blood samples

Blood samples were obtained from two unaffected healthy control subjects and 38 homozygous FRDA subjects. All were enrolled in parallel in an ongoing natural history study at the Children's Hospital of Philadelphia. Written informed consent was obtained from each donor participating in the study. If subjects

were under the age of 18, written informed consent was obtained from a parent or legal guardian. The study was approved by the Institutional Review Board (IRB) of the Children Hospital of Philadelphia (IRB Protocol # 01-002609). Venous blood was drawn in 8.5 mL purple cap Vacutainer EDTA tubes and gently inverted to mix. All samples were immediately aliquoted to Eppendorf tubes and frozen at  $-80\text{ }^{\circ}\text{C}$  until analysis.

### Expression and purification of unlabeled and stable isotope-labeled frataxin-M

The expression of unlabeled and stable isotope labeling by amino acids in cell culture (SILAC)-labeled mature frataxin was performed in *Escherichia coli* BL21 DE3 as described previously.<sup>15</sup> Briefly, the coding sequence of human mature frataxin (81-210) was amplified from FXN cDNA plasmid (pTL1), then cloned into a pET21b plasmid and linked to the 6 $\times$  histidine (His) sequence. The 6 $\times$  His-tag fusion of frataxin was expressed in *Escherichia coli* BL21 DE3 in M9 media containing 1 mM  $\text{MgSO}_4$ , 10  $\mu\text{M}$   $\text{CaCl}_2$ , and 0.5% glucose with 100 mg/L ampicillin. For expressing unlabeled frataxin, the M9 medium was supplemented with 0.025% leucine. For expressing SILAC-labeled frataxin, the M9 medium was supplemented with 0.025% [ $^{13}\text{C}_6$ ]-leucine. The cell pellets were collected and lysed in lysis buffer (50 mM Tris-HCl (pH 8.0), 500 mM NaCl, 10 mM imidazole, 10% glycerol, 2 mM  $\beta$ -mercaptoethanol, 2x protease inhibitor mix, 1 mM PMSF) containing 100  $\mu\text{g}/\text{mL}$  human lysozyme. The lysate was centrifuged at 20,000  $\times$  g for 30 minutes at 4  $^{\circ}\text{C}$ , and the supernatant was purified with Ni-NTA resin. The purity of the unlabeled frataxin-M and SILAC-labeled frataxin-M was confirmed to be >95% by SDS-PAGE and Coomassie blue staining.

### Whole blood sample preparation before IP

All blood samples were thawed at room temperature, and 500  $\mu\text{L}$  of each sample was mixed with 750  $\mu\text{L}$  of NP-40 lysis buffer (150 mM NaCl, 50 mM Tris-HCl pH 7.5, 0.5% Triton X-100, 0.5% NP-40, 1 mM DTT, 1 mM EDTA) containing protease inhibitor cocktail. The same amount of SILAC-labeled frataxin-M (20 ng) was spiked into each sample (calibrator, QC, and whole blood) as an internal standard. Samples were lysed by probe sonication on ice for 30 pulses at power 5 using a sonic dismembrator (Fisher, Pittsburgh, PA), followed by centrifugation at 17,000 g for 15 minutes at 4  $^{\circ}\text{C}$ . The supernatant was transferred from the pellet and incubated with premade DMP-crosslinked anti-frataxin protein G Dynabeads for immunoprecipitation (IP).

### Immunoprecipitation (IP) and Asp-N digestion

Mouse monoclonal anti-frataxin antibody (4  $\mu\text{g}$ ) was cross-linked to protein G beads (0.5 mg) through DMP, as described previously.<sup>15</sup> Briefly, mouse monoclonal anti-frataxin antibody was first incubated with protein G magnetic Dynabeads overnight at 4  $^{\circ}\text{C}$  to form the antibody-coupled beads. The mAb-coupled beads were incubated with 13 mg/mL DMP solution for 1 hour at room temperature to form the stable cross-linked anti-frataxin protein G magnetic Dynabeads. The cross-linked protein G beads can be kept in PBS at 4  $^{\circ}\text{C}$  for 1 week. Processed whole blood samples (1.25 mL) were added into 0.5 mg of anti-frataxin protein G magnetic Dynabeads to carry out IP at 4  $^{\circ}\text{C}$  overnight under rotary agitation. The beads were washed with PBS with 0.02% Tween-20 three times and frataxin-M was eluted with 100  $\mu\text{L}$  of elution buffer (100 mM aqueous acetic acid containing 10% acetonitrile). Eluates were transferred to deactivated glass

inserts (Waters, Milford, MA) and dried in a vacuum concentrator (Jouan RC 10.22, Fisher, Pittsburgh, PA). Samples were dissolved in 50  $\mu$ L of 25 mM aqueous ammonium bicarbonate containing 100 ng of Asp-N and incubated at 37 °C overnight before LC/MS analysis.

### LC/MS analysis

Standard flow ultra-high performance liquid chromatography with multiple reaction monitoring mass spectrometer (UHPLC-MRM/MS) analysis was conducted using a 6495 triple quadrupole LC/MS system coupled to an Agilent 1290 Infinity II LC system. The LC conditions are shown in Table 1, in detail. The nanoflow ultra-high performance liquid chromatography with parallel reaction monitoring mass spectrometer (UHPLC-PRM/MS) analysis was conducted using a third party trap-and-elute nanoflow LC system coupled with a high-resolution orbital trapping mass spectrometer in (PRM) acquisition mode. The UHPLC-PRM/MS conditions are shown in Table 2.

### Data analysis

Data analysis was performed using Skyline (MacCoss Laboratory, University of Washington, Seattle, WA). The peak area ratio of each MRM or PRM transition for each unlabeled/light (L) peptide to labeled/heavy (H) peptide was calculated by the Skyline software and used for absolute quantification. The peptide ratios were calculated by the L/H ratios of the PRM transition of the  $y_4^+$  ion of the S<sup>81</sup>GTLGHPGSL<sup>90</sup> Asp-N peptide

and the  $y_8^+$  ion of the D<sup>198</sup>LSSLAYS<sup>208</sup> Asp-N peptide. Frataxin-M amounts were calculated from the standard curves for each peptide. Frataxin-M levels were then calculated from the average concentrations obtained for the two peptides. The three other

peptides were monitored to provide additional confirmation that frataxin-M was present. Correlations between GAA repeats and frataxin levels were conducted using the linear regression model in Prism 9 for macOS Version 9.3.1 (GraphPad Software, LLC).

**Table 1.** UHPLC-MRM/MS conditions.

Agilent 1290 Infinity II LC Conditions	
Analytical Column	Agilent ZORBAX RRHD Rapid Resolution HD, 2.1 × 50 mm, 1.8 $\mu$ m (p/n 959757-902)
Column Temperature	35 °C
Solvent A	Water, 0.1% formic acid
Solvent B	Acetonitrile, 0.1% formic acid
Analytical LC Flow Rate	0.4 mL/min
Gradient	5% B at 0 min 10% B at 1.00 min 24% B at 2.75 min 36% B at 3.50 min 95% B at 5.00 min 95% B at 6.50 min 5% B at 7.00 min 5% B at 8.50 min
Injection Volume	2 $\mu$ L
Injector Temperature	4 °C
Needle Wash	5 s flush
Needle Wash Solvent	30% methanol
Agilent 6495 LC/TQ Conditions	
Gas Temperature	230 °C
Gas Flow	13 L/min
Ion Polarity	Positive
Nebulizer	40 psi
Sheath Gas Temperature	300 °C
Sheath Gas Flow	10 L/min
Capillary Voltage	4,500 V
Nozzle Voltage	500 V

## Results and discussion

### Sample preparation

During method development, it was found that immunoprecipitation using covalent linkage of the anti-frataxin mouse mAb to magnetic Dynabeads was necessary for the analysis of low abundance protein frataxin-M in whole blood samples. The linkage to Dynabeads served to minimize background interference from high-abundance proteins. In addition, due to the variation during sample enrichment and protease digestion, the use of labeled peptide internal standards after a protease digest step would be inadequate for precise and accurate protein quantification. Therefore, light and heavy stable isotope-labeled frataxin-M proteins were prepared and purified, respectively. Incorporation of the heavy leucine in the heavy-labeled frataxin-M protein was >99.0%. The purified heavy labeled frataxin-M proteins were spiked into blood samples before the IP step as an internal control. The whole experimental workflow is illustrated in Figure 2.

**Table 2.** Nanoflow UHPLC-PRM/MS conditions.

Nanoflow UHPLC Conditions	
Trapping Column	Acclaim PepMap C18 cartridge, 0.3 mm × 5 mm, 100 Å (Thermo Scientific)
Analytical Column	C18 AQ capillary column with a 10 µm pulled tip, 75 µm × 25 cm, 3 µm particle size (ColumnTip, New Haven, CT).
Column Temperature	25 °C
Loading Solvent	Water/acetonitrile (99.5:0.5; v/v) containing 0.1% formic acid
Solvent A	Water/acetonitrile (99.5:0.5; v/v) containing 0.1% formic acid
Solvent B	Acetonitrile/water (98.0:2.0, v/v) containing 0.1% formic acid
Load on trapping column	10 µL/min for 4 min
Analytical LC Flow Rate	400 nL/min
Gradient	2% B at 0 min 2% B at 10 min 35% B at 30 min 60% B at 35 min 98% B at 53 min 80% B at 73 min 2% B at 74 min 2% B 100 min
Injection Volume	8 µL
Injector Temperature	4 °C
Needle Wash	5 s
Needle Wash Solvent	10% methanol
Orbital Trapping Mass Spectrometer Conditions	
Spray Voltage	2,500 V
Ion transfer Capillary Temperature	275 °C
Ion Polarity	Positive
S-lens Rf level	55
I-source CID	2.0 eV
Resolution	60,000
AGC target	2.00E+05
Maximum IT	80 ms

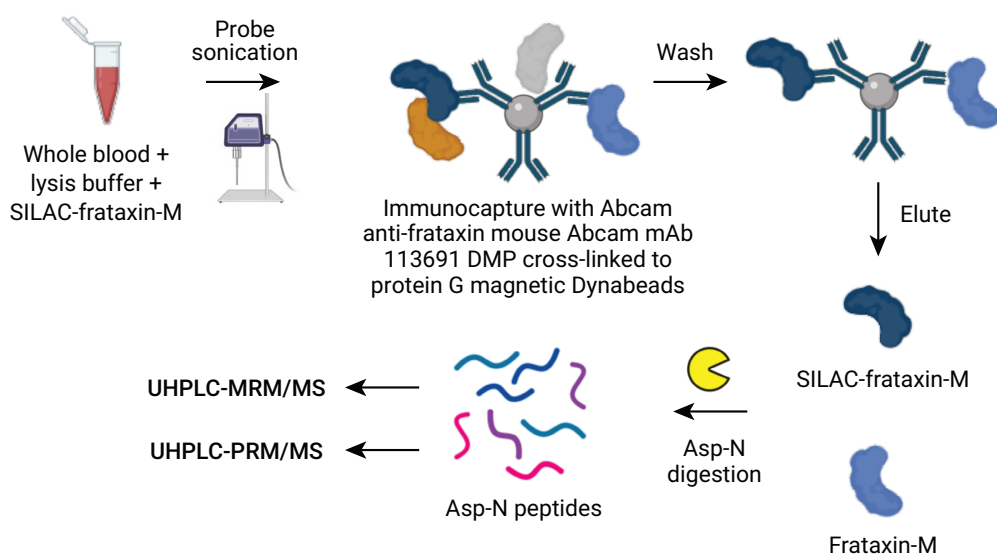


**Figure 2.** Schematic diagram of experimental workflow for frataxin-M sample preparation and LC/MS analysis.

### MRM versus PRM transitions

The monitored peptide sequence from frataxin-M proteins, their corresponding MRM and PRM transitions, as well as the peptide elution time on the two LC/MS systems are shown in Table 3.

For UHPLC-MRM/MS, nominal masses were used for both parent and product ions. In contrast, for UHPLC-PRM/MS, nominal masses were used for the parent ions but accurate masses were used for the product ions. Although in principle the unit-mass LC/TQ system might have some background interference compared to a high-resolution LC/MS system, this problem was not observed for blood frataxin-M analysis on the 6495 LC/TQ. Therefore, after initial protein discovery and method development, the much faster UHPLC-MRM/MS approach was evaluated in terms of quantification accuracy and precision for routine analysis.

### Peptide separation

The Asp-N-digested peptide used for frataxin-M quantification (SGTLGHPGSL) and total frataxin quantification (DLSSLAYS GK) as well as the other three peptides (DETTYERLAEETL, DGVSLHELLAAELTKALKTKL, and

DSLAEFFE) for detection confirmation were well separated from each other. The separation used both standard

flow UHPLC-MRM/MS and nanoflow UHPLC-PRM/MS methods (Figure 3).

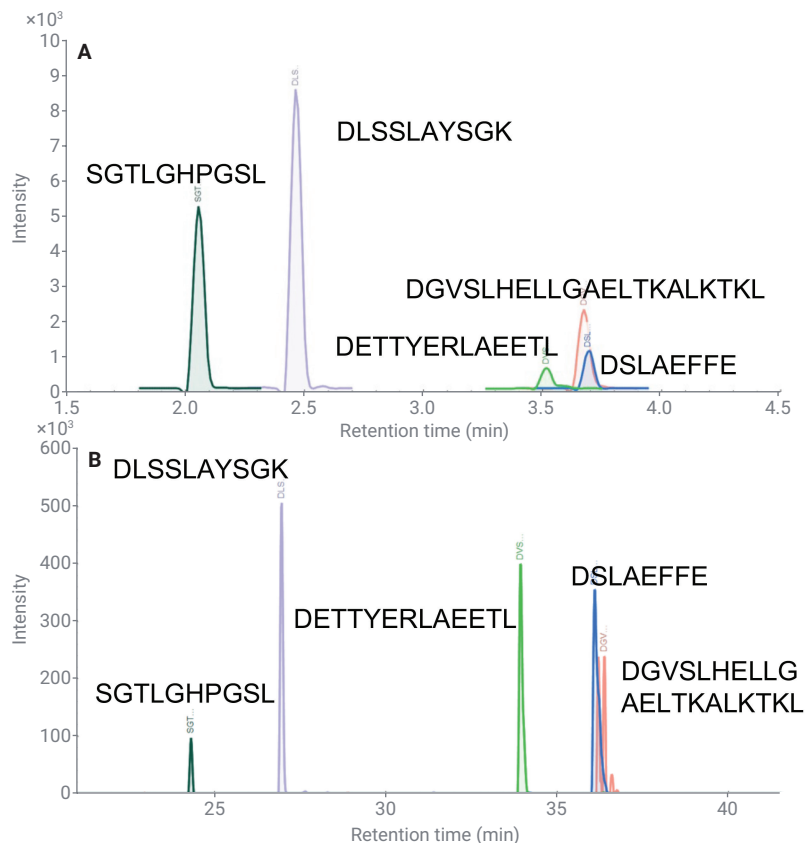


**Figure 3.** LC/MS chromatograms of target peptides: S<sup>91</sup>GTGHPGSL<sup>90</sup> (peptide-1), D<sup>198</sup>LSSLAYS GK<sup>208</sup> (peptide-2), D<sup>91</sup>ETTYERLAEETL<sup>103</sup> (peptide-3), D<sup>178</sup>GVSHELLAAELTKALKTKL<sup>198</sup> (peptide-4), D<sup>104</sup>SLAEFFE<sup>111</sup> (peptide-5). (A) Standard flow UHPLC-MRM/MS. (B) nanoflow UHPLC-PRM/MS.

**Table 3.** MRM/MS and PRM/MS transitions for frataxin-M analysis. Quantification was conducted with shaded peptides and nominal masses were used for MRM/MS. L = [<sup>13</sup>C<sub>6</sub>]-leucine, L = light, H=heavy.

No.	Start	End	Peptide	L or H	Parent Ion	Parent Ion (m/z)	Product Ion 1	Product Ion 1 (m/z)	Product Ion 2	Product Ion 2 (m/z)	Product Ion 3	Product Ion 3 (m/z)	RT UHPLC (min)	RT Nano-UHPLC (min)
1	81	90	SGTLGHPGSL	L	MH <sub>2</sub> <sup>2+</sup>	463.24	y <sub>7</sub> <sup>+</sup>	680.373	y <sub>6</sub> <sup>+</sup>	567.289	y <sub>4</sub> <sup>+</sup>	373.208	2.02	24.05
1	81	97	SGTLGHPGSL	H	MH <sub>2</sub> <sup>2+</sup>	469.26	y <sub>7</sub> <sup>+</sup>	692.413	y <sub>6</sub> <sup>+</sup>	573.309	y <sub>4</sub> <sup>+</sup>	379.229	2.02	24.05
2	198	208	DLSSLAYS GK	L	MH <sub>2</sub> <sup>2+</sup>	520.77	y <sub>8</sub> <sup>+</sup>	812.415	y <sub>7</sub> <sup>+</sup>	725.383	y <sub>3</sub> <sup>+</sup>	291.166	2.44	26.85
2	198	208	DLSSLAYS GK	H	MH <sub>2</sub> <sup>2+</sup>	527.79	y <sub>8</sub> <sup>+</sup>	818.435	y <sub>7</sub> <sup>+</sup>	731.403	y <sub>3</sub> <sup>+</sup>	291.166	2.44	26.85
3	91	103	DETTYERLAEETL	L	MH <sub>3</sub> <sup>3+</sup>	523.91	b <sub>12</sub> <sup>**</sup>	719.820	b <sub>11</sub> <sup>**</sup>	669.296	b <sub>10</sub> <sup>**</sup>	604.775	3.26	32.25
3	91	103	DETTYERLAEETL	H	MH <sub>3</sub> <sup>3+</sup>	527.93	b <sub>12</sub> <sup>**</sup>	722.830	b <sub>11</sub> <sup>**</sup>	672.307	b <sub>10</sub> <sup>**</sup>	607.785	3.26	32.25
4	178	198	DGVSLHELLAAELTKALKTKL	L	MH <sub>4</sub> <sup>4+</sup>	563.33	y <sub>12</sub> <sup>**</sup>	643.906	y <sub>11</sub> <sup>**</sup>	608.387	b <sub>2</sub> <sup>+</sup>	173.056	3.66	37.05
4	178	198	DGVSLHELLAAELTKALKTKL	H	MH <sub>4</sub> <sup>4+</sup>	563.33	y <sub>12</sub> <sup>**</sup>	652.936	y <sub>11</sub> <sup>**</sup>	617.417	b <sub>2</sub> <sup>+</sup>	173.056	3.66	37.05
5	104	111	DSLAEFFE	L	MH <sub>2</sub> <sup>2+</sup>	479.21	b <sub>4</sub> <sup>+</sup>	387.187	b <sub>3</sub> <sup>+</sup>	316.150	y <sub>2</sub> <sup>+</sup>	295.129	3.68	36.05
5	104	111	DSLAEFFE	H	MH <sub>2</sub> <sup>2+</sup>	482.22	b <sub>4</sub> <sup>+</sup>	393.208	b <sub>3</sub> <sup>+</sup>	316.150	y <sub>2</sub> <sup>+</sup>	295.129	3.68	36.05

The MS signals were adequate on both systems for detection and quantification, although less sample (2  $\mu$ L, Table 1) was injected on the MRM/MS system than on the PRM/MS system (8  $\mu$ L, Table 2). Standard curves were linear in the range of 0.5 to 60 ng for SGTLGHPGSL ( $MH_2^{2+} \rightarrow y_4^+$ ) and DLSSLAYSGK ( $MH_2^{2+} \rightarrow y_8^+$ ). The curve had an  $R^2$  of 0.9985 and 0.9985, respectively on the standard flow UHPLC-MRM/MS system (Figure 4A). The curve from the nanoflow UHPLC-PRM/MS system had an  $R^2$  of 0.9622 and 0.9951, respectively (Figure 4B). The standard curves acquired from the 6495 LC/TQ systems show better precision and accuracy compared to those from the nanoflow UHPLC-PRM/MS system. The results showed a better LOD and LOQ for both peptides on the standard flow UHPLC-MRM/MS system (Figure 4).

There was also a dramatic difference in the run times with all five peptides eluting within 4 minutes on the standard flow UHPLC system compared to 38 minutes on the nanoflow UHPLC (Figure 3). These run times translated to an overall individual run times of 11 minutes on the standard flow UHPLC system and 105 minutes on the nanoflow UHPLC system (Figure 5). A typical assay for frataxin-M includes 10 standards and 30 blood samples from FRDA subjects. The time taken to analyze these samples in triplicate was 23 hours on standard flow UHPLC-MRM/MS compared to 8 days, 18 hours on nanoflow UHPLC-PRM/MS systems (Figure 5). The significant reduction in instrument run time and high quantification quality using the standard flow UHPLC-MRM/MS also allowed for the completion of several other high-through frataxin studies in the lab.<sup>11,12</sup>

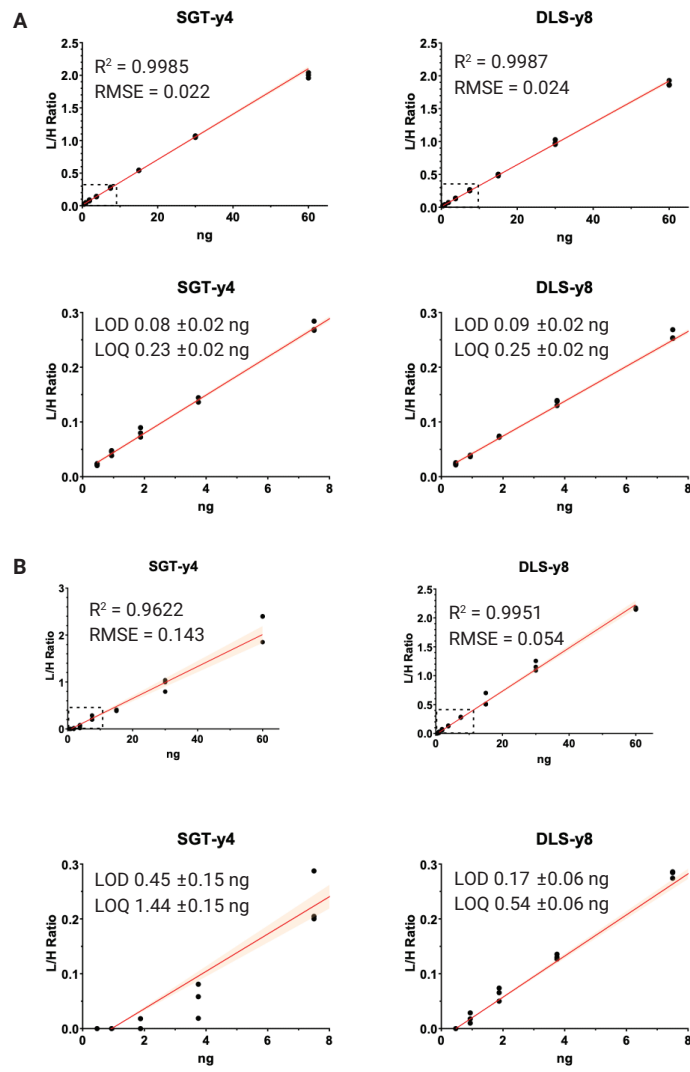


**Figure 4.** Calibration curves for peptides SGTLGHPGSL.D ( $MH_2^{2+} \rightarrow y_4^+$ ) and L.DLSSLAYSGK.D ( $MH_2^{2+} \rightarrow y_8^+$ ). (A) UHPLC-MRM/MS. (B) nanoflow UHPLC-PRM/MS. Upper plots show calibration curves with correlation coefficients ( $R^2$ ) and root mean square error (RMSE) for levels ranging 0 to 80 ng, lower plots show calibration curves for the lower levels ranging 0 to 8 ng with their corresponding LOD and LOQ.

## Healthy control and FRDA subjects blood samples

Blood levels of frataxin-M in two healthy controls, were 4.5 and 5.2 ng/mL, respectively (Figure 6), which is like the levels found in previous studies. In contrast, the blood frataxin-M levels found in FRDA subjects were in the range 0.3 to 3.8 ng/mL. The highest concentration found in the FRDA subject samples was from a subject with a mean of only 200 GAA repeats, consistent with a milder form of the disease. The lowest concentration was from a subject with a mean of 1,000 GAA repeats, consistent with the most severe form of the disease. Interestingly, there was a good correlation ( $R^2 = 0.8547$ ) between frataxin-M levels and mean GAA repeats (Figure 6). This correlation is consistent with what was found previously using the nanoflow UHPLC-PRM/MS.<sup>13</sup> The intercept of the Y-axis corresponds to the mean frataxin-M levels found in blood from healthy control subjects.

## Conclusion

An immunoprecipitation (IP) method was developed using the covalently linked anti-frataxin mouse mAb to enrich frataxin proteoforms in whole blood samples. Stable isotope-labeled heavy frataxin-M protein was spiked into the blood samples prior to IP step as an internal standard. All the IP samples were then digested with Asp-N protease. A nanoflow UHPLC-PRM/MS system was initially used for target peptide quantification. Afterwards, a much faster standard flow UHPLC-MRM/MS method was developed using an Agilent 6495 LC/TQ system without the need for on-column sample concentration. This application note shows the analytical performance comparison

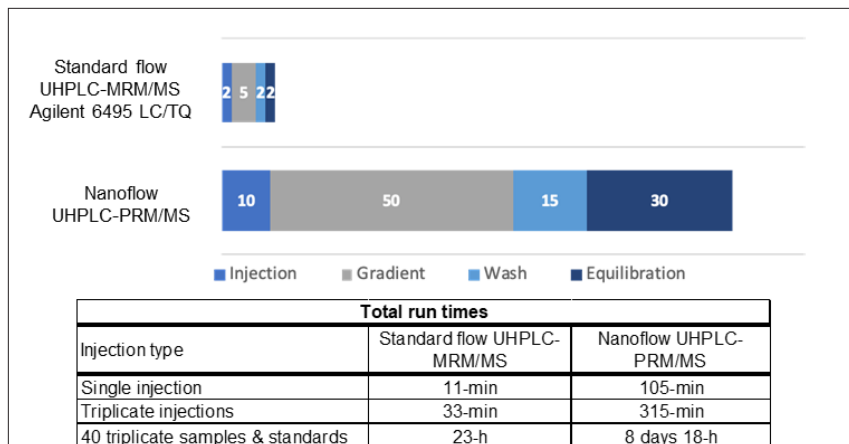


**Figure 5.** Comparison of LC/MS run time between standard flow UHPLC-MRM/MS and nanoflow UHPLC-PRM/MS methods. For both methods, three washes were included (starting after calibration and after samples).

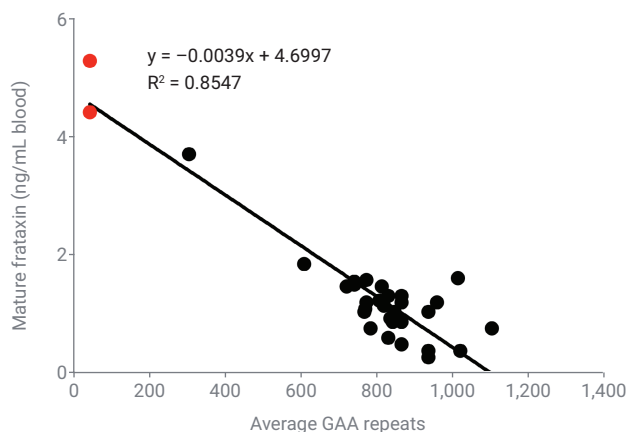


**Figure 6.** Human frataxin-M concentrations in blood samples were highly correlated with average GAA repeats in the gene of disease subjects based on the Agilent 6495 LC/TQ analysis results. Healthy control subjects are in red.

between these two LC/MS systems for frataxin-M protein quantification in whole blood samples. The much faster method, excellent linearity, precision, and accuracy using the 6495 LC/TQ system allowed replacement of the previous nanoflow UHPLC-PRM/MS method with the much faster standard flow UHPLC-MRM/MS method.



## References

1. Evans-Galea, M. V. *et al.* Cell and Gene Therapy for Friedreich Ataxia: Progress to Date. *Hum. Gene Ther.* **2014**, *25*(8), 684–93. Epub 2014/04/23. doi: 10.1089/hum.2013.180. PubMed PMID: 24749505.
2. Pousset, F. *et al.* Durr A. A 22-Year Follow-up Study of Long-term Cardiac Outcome and Predictors of Survival in Friedreich Ataxia. *JAMA Neurol.* **2015**, *72*(11), 1334–41. Epub 2015/09/29. doi: 10.1001/jamaneurol.2015.1855. PubMed PMID: 26414159.
3. Lynch, D. R. *et al.* Safety, Pharmacodynamics, and Potential Benefit of Omaveloxolone in Friedreich Ataxia. *Ann. Clin. Transl. Neurol.* **2019**, *6*(1), 15–26. Epub 2019/01/19. doi: 10.1002/acn3.660. PubMed PMID: 30656180; PMCID: PMC6331199.
4. Santos, R. *et al.* Friedreich Ataxia: Molecular Mechanisms, Redox Considerations, and Therapeutic Opportunities. *Antioxid. Redox. Signal.* **2010**, *13*(5), 651–90. Epub 2010/02/17. doi: 10.1089/ars.2009.3015. PubMed PMID: 20156111; PMCID: PMC2924788.
5. Gellera, C. *et al.* Frataxin Gene Point Mutations in Italian Friedreich Ataxia Patients. *Neurogenetics* **2007**, *8*(4), 289–99. Epub 2007/08/19. doi: 10.1007/s10048-007-0101-5. PubMed PMID: 17703324.
6. Sacca, F. *et al.* A Combined Nucleic Acid and Protein Analysis in Friedreich Ataxia: Implications for Diagnosis, Pathogenesis and Clinical Trial Design. *PLoS One* **2011**, *6*(3), e17627. Epub 2011/03/18. doi: 10.1371/journal.pone.0017627. PubMed PMID: 21412413; PMCID: PMC3055871.
7. Rotig, A. *et al.* Aconitase and Mitochondrial Iron-Sulphur Protein Deficiency in Friedreich Ataxia. *Nat. Genet.* **1997**, *17*(2), 215–7. doi: 10.1038/ng1097-215. PubMed PMID: 9326946.
8. Delatycki, M. B.; Bidichandani, S. I. Friedreich Ataxia- Pathogenesis And Implications for Therapies. *Neurobiol Dis.* **2019**, *132*, 104606. Epub 20190905. doi: 10.1016/j.nbd.2019.104606. PubMed PMID: 31494282.
9. Doni, D. *et al.* The Displacement of Frataxin from the Mitochondrial Cristae Correlates with Abnormal Respiratory Supercomplexes Formation and Bioenergetic Defects in Cells of Friedreich Ataxia Patients. *FASEB J.* **2021**, *35*(3), e21362. doi: 10.1096/fj.202000524RR. PubMed PMID: 33629768.
10. Monfort, B. *et al.* Recent Advances in the Elucidation of Frataxin Biochemical Function Open Novel Perspectives for the Treatment of Friedreich's Ataxia. *Front Neurosci.* **2022**, *16*, 838335. Epub 20220302. doi: 10.3389/fnins.2022.838335. PubMed PMID: 35310092; PMCID: PMC8924461.
11. Guo, L. *et al.* Characterization of a New N-Terminally Acetylated Extra-Mitochondrial Isoform of Frataxin in Human Erythrocytes. *Sci. Rep.* **2018**, *8*(1), 17043. Epub 2018/11/20. doi: 10.1038/s41598-018-35346-y. PubMed PMID: 30451920; PMCID: PMC6242848.
12. Rodden, L. N. *et al.* DNA Methylation in Friedreich Ataxia Silences Expression of Frataxin Isoform E. *Sci. Rep.* **2022**, *12*(1), 5031. Epub 20220323. doi: 10.1038/s41598-022-09002-5. PubMed PMID: 35322126; PMCID: PMC8943190.
13. Wang, Q. *et al.* Simultaneous Quantification of Mitochondrial Mature Frataxin and Extra-Mitochondrial Frataxin Isoform E in Friedreich's Ataxia Blood. *Front. Neurosci.* **2022**, *16*, 874768. Epub 20220428. doi: 10.3389/fnins.2022.874768. PubMed PMID: 35573317; PMCID: PMC9098139.
14. Blair, I. A. *et al.* The Current State of Biomarker Research for Friedreich's Ataxia: a Report from the 2018 FARA Biomarker Meeting. *Future Sci. OA.* **2019**, *5*(6), FSO398. Epub 2019/07/10. doi: 10.2144/fsoa-2019-0026. PubMed PMID: 31285843; PMCID: PMC6609901.
15. Guo, L. *et al.* Liquid Chromatography-High Resolution Mass Spectrometry Analysis of Platelet Frataxin as a Protein Biomarker for the Rare Disease Friedreich's Ataxia. *Anal. Chem.* **2018**, *90*(3), 2216–23. Epub 2017/12/23. doi: 10.1021/acs.analchem.7b04590. PubMed PMID: 29272104; PMCID: PMC5817373.

[www.agilent.com](http://www.agilent.com)

For Research Use Only. Not for use in diagnostic procedures.

RA44930.5725

This information is subject to change without notice.

© Agilent Technologies, Inc. 2023  
Printed in the USA, January 26, 2023  
5994-5608EN

